Title

Ephrin-B2 overexpression predicts for poor prognosis and response to therapy in solid tumors.

Journal

Molecular Carcinogenesis, 56(3)

Authors

Oweida, Ayman
Bhatia, Shilpa
Hirsch, Kellen
et al.

Publication Date

2017-03-01

DOI

10.1002/mc.22574

Peer reviewed

HHS Public Access

Author manuscript

Mol Carcinog. Author manuscript; available in PMC 2018 May 08.

Published in final edited form as:

Mol Carcinog. 2017 March ; 56(3): 1189–1196. doi:10.1002/mc.22574.

Ephrin-B2 Overexpression Predicts for Poor Prognosis and Response to Therapy in Solid Tumors

Ayman Oweida[1], **Shilpa Bhatia**[1], **Kellen Hirsch**[1], **Dylan Calame**[1], **Anastacia Griego**[1], **Steve Keysar**[2], **Todd Pitts**[3], **Jaspreet Sharma**[1], **Gail Eckhardt**[3], **Antonio Jimeno**[2], **Xiao Jing Wang**[4], **Gill Parkash**[5,6], **Joseph Califano**[7], and **Sana D. Karam**[1,*]

[1]Department of Radiation Oncology, Anschutz Medical Campus, University of Colorado Denver, Denver, Colorado

[2]Department of Oncology, Anschutz Medical Campus, University of Colorado Denver, Denver, Colorado

[3]Division of Medical Oncology, Anschutz Medical Campus, University of Colorado Denver, Denver, Colorado

[4]Department of Pathology, Anschutz Medical Campus, University of Colorado Denver, Aurora, Colorado

[5]Vasgene Therapeutics, Los Angeles, California

[6]Department of Oncology, University of Southern California, Los Angeles, Southern California

[7]Department of Otolaryngology, University of Southern California, San Diego, Southern California

Abstract

Ephrin B2 is variably expressed on tumor cells and its blockade has been shown to inhibit angiogenesis in animal models of pancreatic, colorectal, lung and head, and neck squamous cell carcinomas. However, the implications of ephrinB2 expression in cancer patients have remained elusive. In this study, we analyzed the cancer genome atlas (TCGA) for ephrinB2 expression. We report significant correlations between EFNB2 expression, overall survival and disease-free survival in head and neck squamous cell carcinoma (HNSCC, $n = 519$), pancreatic adenocarcinoma ($n = 186$), and bladder urothelial carcinoma ($n = 410$). In HNSCC patients, high-EFNB2 mRNA expression was associated with tumor HPV negativity, oral cavity location, alcohol intake, higher TP53 mutation, and EGFR amplification. EphrinB2 overexpression also correlated with worse response to chemotherapy and radiotherapy. The therapeutic potential of blocking ephrinB2 was validated in HNSCC patient-derived tumor xenografts and showed significant improvement in survival and tumor growth delay. Our data shows that ephrinB2 overexpression can serve as a critical biomarker for patient prognosis and response to therapy. These results should guide design of future clinical trials exploring EphrinB2 inhibition in cancer patients.

*Correspondence to: Department of Radiation Oncology, Anschutz Medical Campus, University of Colorado Denver, Denver, CO.

Conflict of interest: The authors have declared that no conflict of interest exists.

SUPPORTING INFORMATION

Additional supporting information may be found in the online version of this article at the publisher's web-site.

Keywords

cancer; ephrin; chemotherapy; radiation therapy

INTRODUCTION

Ephrins represent a class of membrane-bound ligands that regulate an array of cellular and physiological functions including axon guidance [1–3], angiogenesis [4,5], lymphatic valve development [6], and epithelial cell migration [7]. Ephrins and their corresponding Eph receptors are divided into A and B classes based on their structure, ligand affinity, and membrane-linkage. Ephrins exert their biological functions by binding to Eph receptors, which comprise the largest family of receptor tyrosine kinases. In addition to Eph/Ephrin signaling, ephrins can act in an Eph-receptor-independent manner through reverse signaling [8,9]. Reverse signaling occurs when the cytoplasmic ephrin domain is phosphorylated resulting in activation of cell signaling pathways [10–13]. Both Eph/Ephrin signaling have been implicated in cancer development and progression (reviewed in [14,15]). In particular, ephrins have been shown to be important mediators of tumor cell invasion, migration, and angiogenesis [16–19]. Several groups have shown ephrin-B2 to be a poor prognostic indicator in a variety of tumors including ovarian, uterine endometrial cancers, esophageal squamous cell carcinoma, and astrocytoma [17,20,21]. However, most studies to date have been limited by small population size and absence of a clear biomarker of therapeutic potential.

The cancer genome atlas (TCGA) comprises a database of over 10,000 primary tumors categorized based on cancer type and containing data related to gene expression, gene copy number amplification, mutation status, methylation status as well as response to chemo, and radiotherapy. We hypothesized that overexpression of the ephrin B2 gene (EFNB2) selects for patients with poor survival and poor response to therapy in the TCGA. We also hypothesized that EFNB2 blockade can inhibit tumor growth and improve survival in patient-derived xenograft (PDX) tumor models.

MATERIALS AND METHODS

Patient Tissue

Tissue samples were collected from the Johns Hopkins Tissue Core, part of the Head and Neck Cancer Specialized Program of Research Excellence (HNC-SPORE). All patients were recruited under an institutional review board approved protocol.

RNA Preparation and Sequencing

For gene-expression profiling of patient samples, RNA was extracted from 0.35 mm thick frozen tissue sections using the mirVana miRNA Isolation Kit (Ambion, Forster City, CA) per manufacturer’s recommendations. The concentration of RNA was quantified using a NanoDrop spectrophotometer (Thermo Fisher Scientific, Waltham, MA). The RNA quality was assessed using an Agilent RNA 6000 Nano Kit (Santa Clara, CA). The samples were required to achieve an RNA Integrity Number (RIN) of at least 7.0. After RNA extraction,

47 tumors and 25 normal samples passed minimum quality thresholds. A stranded RNA library was prepared using the Illumina TruSeq stranded total RNA seq poly A1 Gold kit (San Diego, CA) following the manufacturer's recommendations. Next, a ribosomal RNA reduction was performed from 400 ng of total RNA and purified with AMPure XP magnetic beads. The purified RNA was fragmented and converted to double stranded cDNA, and the cDNA was 3′ adenylated and ligated with barcode adapters. The library was then enriched using PCR and AMPure XP bead purification. The quality and quantity of each library was assessed using the Agilent High Sensitivity DNA Analysis Kit. Sequencing was performed using the HiSeq 2500 platform sequencer (Illumina), and the TruSeq Cluster Kit for 2 × 100 bp sequencing. RNA sequencing data were normalized using the version 2 protocols as developed by TCGA.10. The RNA sequences were aligned to the GRCh37/hg19 genome assembly using MapSplice2 version 2.0.1.9. MapSplice was run with the default command line arguments and the fusion option to perform fusion identification and quantify read counts in fusions during the alignment.

Protein Expression

For analysis of protein expression in patient samples, HNSCC and pancreatic tumor tissue was obtained from the labs of Drs. Antonio Jimeno and Gail Eckhardt (University of Colorado, Anschutz Medical Campus). Tissue was snap-frozen at the time of surgery and stored in −80°C. At the time of lysate collection, tissue was placed in liquid nitrogen and with the aid of a pestle made into fine powder. Radio-immunoprecipitation assay buffer (RIPA buffer) was used to lyse the tissue. Protein concentration was determined using the BCA assay.

Patient-Derived Xenograft Tumor Model

Female athymic nude mice (5–6-wk-old) were purchased from Harlan Laboratories. All mice were maintained, handled, and euthanized in accordance with the ethics guidelines and conditions set by the University of Colorado, Anschutz Medical Campus Animal Care, and Use Committee. Early passage (F8-F12) HNSCC PDX tumor tissues were obtained from Dr. Antonio Jimeno's lab (University of Colorado, Anschutz Medical Campus). For implantation, tumors were placed in collecting medium consisting of RPMI supplemented with 10% fetal bovine serum (FBS), 200 U/mL penicillin, and 200 μg/mL streptomycin, and cut into 3 × 3 × 3 mm pieces. Up to 20 mice (40 tumors) were implanted in each experiment. The right and left hind flanks were sterilized and small incisions on the right and left hind flank were made to create subcutaneous pockets. Tumor pieces prepared in 3 × 3 × 3 mm size were immersed in Matrigel (BD Biosciences, San Jose, CA) and inserted into the subcutaneous pocket. Tumor growth was measured using a digital caliper. Tumor volume was calculated using the following ellipsoid formula: ([smaller diameter)^2×[longer diameter])/2. When tumor volumes reached a size of approximately 100–150 mm^3, the mice were randomized to PBS or sEphB4-HSA. Mice were either injected with PBS or administered with 20 mg/kg dose of sEphB4-HSA intraperitoneally (three times/week) throughout the course of the experiment.

Antibodies and Reagents

Protein extracts (30 μg) were loaded onto 10% SDS–PAGE gels. Electrophoresis, blocking, probing, and visualization of proteins were conducted as described [17]. Ephrin-B2 was obtained from Abcam (Cambridge, MA), phsopho-EphrinB2 was obtained from Sigma–Aldrich (St. Louis, MO), and beta-actin was obtained from Cell Signaling Technology (Danvers, MA). sEphB4-HSA protein for blocking ephrin B2 was provided by Dr. Gill Parkash (University of Southern California, Los Angeles, CA).

Statistics

Survival analysis and disease-free survival for each cancer was based on average mRNA expression. Overall survival and disease-free survival was calculated by Kaplan–Meier method using log-rank tests for comparisons. Disease-free survival (DFS) was defined as time from the date of diagnosis to the date of the last known occasion that the patient was disease-free, or the date of disease recurrence (local, regional, or distant recurrence). Death without documented recurrence was censored at the date of death. Univariate Cox proportional model was used to calculate the Hazard ratio (HR). Two-sided *P*-values were reported for all survival analyses.

Patient characteristics data were obtained directly from the TCGA. Bivariate analysis of patient and tumor characteristics was performed based on EFNB2 expression. Two-sided Fisher's exact test and the Chi-squared test were applied for bivariate analysis. For the purposes of this study, classifications of alveolar ridge, buccal mucosa, lip, oral tongue, and floor of mouth were re-classified to oral cavity. Tonsil was re-classified to oropharynx.

Multivariate Cox regression analysis for OS and DFS was performed for alcohol, TP53, EGFR, disease site, and EFNB2. For validation of the relationship between HPV status and EFNB2 expression, sequencing data were pooled from patient data available from JHU and the TCGA. One-way analysis of variance (ANOVA) with Tukey correction was applied for statistical analysis. Four stars represent *P*-value <0.0001.

Statistical significance of ephrin-B2 inhibition on tumor growth curves in PDX models was assessed by one-way ANOVA. A *P*-value of 0.05 was considered statistically significant. At the termination of the experiment, tumors were collected and flash-frozen.

All statistical analyses were performed in GraphPad Prism software and SAS software.

RESULTS AND DISCUSSION

We interrogated the TCGA database for mRNA expression of EFNB2 across all cancers (Supplementary Figure S1). High-EFNB2 expression correlated significantly with poor survival in a number of solid cancers, including HNSCC (median OS 27.04 months vs. 68.43) pancreatic adenocarcinoma (median OS 15.80 vs. 22.83 months) and bladder urothelial cancer (median OS 23.19 vs. 44.28 months). In addition, EFNB2 expression correlated with reduced disease-free survival in the same populations (Figure 1). Expression of EFNB2 was significantly higher in tumor tissue compared to normal tissue, which was defined based on data analyzed using oncomine (Supplementary Figure S2). Previous

studies have also shown significantly increased protein levels of EFNB2 in HNSCC tissue compared to normal tissue [22,23]. Additionally, inhibition of EFNB2 signaling in HNSCCs has been shown to result in tumor growth retardation [23]. For further analysis, we therefore focused on the cohort of HNSCC patients. Based on average EFNB2 mRNA expression, 318 patients were classified as having low-EFNB2 expression and 201 patients were classified as having high-EFNB2 expression. Mutation status was available for 134 high EFNB2 patients and 132 low EFNB2 patients. In addition, copy number amplification was available for 201 high EFNB2 patients and 302 low EFNB2 patients.

Figure 2A shows bivariate analysis of the two patient populations based on patient and tumor characteristics. EFNB2 expression correlated significantly with the presence of TP53 mutations ($P = 0.0003$) and EGFR amplification ($P = 0.0126$). Subgroup analysis comparing patients with stage T1–T2 and stage T3–T4 tumors (according to the neoplasm American Joint Committee on Cancer clinical primary tumor T stage) revealed a significant difference in OS in patients with high-EFNB2 expression compared to patients with low-EFNB2 expression (Figure 2B). Median OS for stage T1–T2 patients with high EFNB2 was 35.51 months compared to 57.88 months for stage T1–T2 patients with low-EFNB2 expression ($P = 0.0019$). In addition, subgroup analysis based on nodal status showed significantly decreased OS and DFS in N1–N2b patients with high-EFNB2 expression compared to N1–N2b patients with low-EFNB2 expression (Figure 2C). Median OS for N1–N2b patients with high EFNB2 was 18.96 months compared to 71.16 months in N1–N2b patients with low EFNB2 ($P = 0.0005$). We further classified the population of HNSCC patients based on disease site. Within the high-EFNB2 patient population, the majority of tumors were seen in the oral cavity (73%) whereas only 17% of oropharynx patients had high-EFNB2 expression. Since the majority of patients (82%) were heavy smokers (>10 pack year history of smoking (as defined by RTOG 0129 [24]), there was no difference by smoking status. However, EFNB2 expression correlated significantly with alcohol consumption frequency ($P = 0.0341$). Multivariate cox regression analysis demonstrated significant correlation between EFNB2 expression and OS as well as DFS (Figure 2D).

We performed further analysis in the TCGA database to investigate associations between EFNB2 expression and primary tumor treatment response. Radiotherapy data (for curative intent) was available for 112 patients with high EFNB2 and 173 patients with low EFNB2 (Figure 3A). Patients treated with RT who had high-EFNB2 expression performed significantly worse compared to patients with low-EFNB2 expression (median survival 35.45 months compared to 88.8 months, $P = 0.0018$, HR = 1.88, HR range = 1.27–2.81). A tendency towards decreased progression-free survival was observed in the high-EFNB2 population (median time to progression 35.0 months compared to 45.0 months, $P = 0.0882$, HR = 1.351, HR range = 1.0–2.01). Chemotherapy data were available for 67 patients with high EFNB2 and 107 patients with low EFNB2 (Figure 3B). The majority of patients received cisplatin chemotherapy (53%), followed by carboplatin (20%), cetuximab (11%), paclitaxel (8%), and 8% received other forms of drug/chemotherapy. Patients with high EFNB2 who were treated with chemotherapy had significantly worse OS (median survival 25.9 months compared to 56.9 months, $P = 0.0087$, HR = 1.94, HR range = 1.2–3.2) and progression-free survival (median time to progression 18.4 months compared to 45.0 months, $P = 0.0397$, HR = 1.66, HR range = 1.03–2.68). These findings provide evidence

that ephrinB2 expression correlates with poor survival, disease-free survival, and poor response to therapy.

Since HPV status is a known and validated prognostic marker in HNSCC, we examined the correlation between EFNB2 expression and HPV status. HPV status based on p16 expression was available for 35 high EFNB2 patients and 72 low EFNB2 patients. The majority (92%) of HPV+ patients (35/38) had low-EFNB2 expression (P <0.0001). Out of the three HPV+ patients with high EFNB2, one was negative for HPV based on in situ hybridization analysis while the there was no ISH data available on the remaining two patients. No additional gender, race, or age differences could be observed. Since the TCGA contains only 39 HPV+ patients, we performed additional validation for EFNB2 expression in an independent cohort of 47 HPV+ HNSCC patients. We pooled sequencing data available from Johns Hopkins University as well as the TCGA for analysis of EFNB2 expression. EphrinB2 expression in HPV− tumors was significantly higher compared to HPV+ tumors as well as normal tissue (Figure 4). No significant difference could be observed in ephrinB2 expression between HPV+ tumors and normal tissue.

To underscore the impact of these findings at the protein level, we next examined EFNB2 protein expression and correlated it with mRNA expression. Frozen tissue samples from HNSCC and pancreatic cancer patients available at our institution were analyzed by western blotting. All patient tumor samples expressed moderate to high levels of EFNB2 protein (Figure 5A). To corroborate, the correlation between mRNA and protein expression, linear regression analysis was conducted on sequencing data obtained from RNAseq on seven HNSCC patient samples and revealed similar patterns of expression to protein levels (R^2 = 0.56, Figure 5B).

To validate the therapeutic potential of blocking EFNB2 we performed in vivo experiments using a PDX from a patient with relapsed oral cavity tumor. Blockade of EFNB2 using sEphB4-HSA (VasGene Therapeutics, Los Angeles, CA) has been previously characterized [25] and shown to have efficacy in Kaposi Sarcoma [26]. In addition, sEphB4-HSA demonstrated efficacy in cancers where sEphB4-HSA/EphrinB2 signaling promotes tumor growth and angiogenesis [27–29]. The drug is comprised of the recombinant soluble extracellular domain of sEphB4-HSA, containing the globular ligand-binding subdomain for ephrinB2. Based on our screening of patient-derived tissue samples, we selected the CUHN004 PDX which showed high EFNB2 expression as revealed by Western blot analysis (Figure 5A) for validation of sEphB4-HSA efficacy. The CUHN004 PDX was derived from an HPV negative patient diagnosed with tumor of the floor of mouth and who relapsed within 3 years after having received surgery, chemotherapy and radiation therapy. Tissue was harvested at the time of relapse. EphrinB2 blockade resulted in significant inhibition of tumor growth in the patient-derived CUHN004 xenograft compared to PBS-treated animals (Figure 5C). For proof of target, western blotting was conducted for total- and phospho-EFNB2. Early time point analysis revealed significant decrease in phosphorylated and total levels of EFNB2 72 h after administration of the first dose of s-EphB4-HSA (Figure 5D).

In this study, we have demonstrated that EFNB2 overexpression correlates with poor survival and disease-free survival in HNSCC, pancreatic adenocarcinoma, and urothelial

bladder carcinoma based on data from over 1100 patients in the TCGA. We chose to focus on the cohort of HNSCC patients due to the presence of a large sample size in both high and low EFNB2 expressing patients. Our data demonstrate that ephrinB2 overexpression not only predicts for worse overall survival outcomes, but also significantly worse response to chemo and radiotherapy. Our data show that EFNB2 over-expression appears to be a driver of poor prognosis in high-risk patients–those with oral cavity cancer, high alcohol consumption, and HPV negative disease. Even with early stage tumors (T1–T2 and N1–N2b) EFNB2 overexpression correlates with worse overall survival outcomes. Blockade of EFNB2 in PDX tumor derived from a patient with relapsed oral cavity caner, inhibited tumor proliferation, and increased animal survival. This striking response potentially represents a prime target for new anti-cancer therapy. These findings should help set the stage to design rational studies and clinical trials aimed at testing EFNB2 inhibition in cohorts of high-risk patients described in this analysis.

Supplementary Material

Refer to Web version on PubMed Central for supplementary material.

Acknowledgments

Grant sponsor: Paul Calabresi Career Development Award for Clinical Oncology (K12); Grant sponsor: American Cancer Society Institutional Grant; Grant sponsor: Cancer League of Colorado; Grant sponsor: Golfer’s grant; Grant sponsor: Pre Head and Neck Spore

This work was supported by the Paul Calabresi Career Development Award for Clinical Oncology (K12), American Cancer Society Institutional Grant, Cancer League of Colorado, Golfer’s grant, and Pre Head and Neck Spore grant.

References

1. Guthrie S. Ephrin cleavage: A missing link in axon guidance. Trends Neurosci. 2000; 23:592. [PubMed: 11137146]
2. Huot J. Ephrin signaling in axon guidance. Prog Neuro-psychopharmacol Biol Psychiatry. 2004; 28:813–818.
3. Reber M, Hindges R, Lemke G. Eph receptors and ephrin ligands in axon guidance. Adv Exp Med Biol. 2007; 621:32–49. [PubMed: 18269209]
4. Mosch B, Reissenweber B, Neuber C, et al. Eph receptors and ephrin ligands: Important players in angiogenesis and tumor angiogenesis. J Oncol. 2010; 2010:135285. [PubMed: 20224755]
5. Sawamiphak S, Seidel S, Essmann CL, et al. Ephrin-B2 regulates VEGFR2 function in developmental and tumour angiogenesis. Nature. 2010; 465:487–491. [PubMed: 20445540]
6. Zhang G, Brady J, Liang WC, et al. EphB4 forward signalling regulates lymphatic valve development. Nat Commun. 2015; 6:6625. [PubMed: 25865237]
7. Miao H, Wang B. Eph/ephrin signaling in epithelial development and homeostasis. Int J Biochem Cell Biol. 2009; 41:762–770. [PubMed: 18761422]
8. Kullander K, Klein R. Mechanisms and functions of Eph and ephrin signalling. Nat Rev Mol Cell Biol. 2002; 3:475–486. [PubMed: 12094214]
9. Thakar S, Chenaux G, Henkemeyer M. Critical roles for EphB and ephrin-B bidirectional signalling in retinocollicular mapping. Nat Commun. 2011; 2:431. [PubMed: 21847105]
10. Holland SJ, Gale NW, Mbamalu G, et al. Bidirectional signalling through the EPH-family receptor Nuk and its transmembrane ligands. Nature. 1996; 383:722–725. [PubMed: 8878483]
11. Bruckner K, Pasquale EB, Klein R. Tyrosine phosphorylation of transmembrane ligands for Eph receptors. Science. 1997; 275:1640–1643. [PubMed: 9054357]

12. Adams RH, Diella F, Hennig S, et al. The cytoplasmic domain of the ligand ephrinB2 is required for vascular morphogenesis but not cranial neural crest migration. Cell. 2001; 104:57–69. [PubMed: 11163240]
13. Cowan CA, Yokoyama N, Saxena A, et al. Ephrin-B2 reverse signaling is required for axon pathfinding and cardiac valve formation but not early vascular development. Dev Biol. 2004; 271:263–271. [PubMed: 15223333]
14. Pasquale EB. Eph receptors and ephrins in cancer: Bidirectional signalling and beyond. Nat Rev Cancer. 2010; 10:165–180. [PubMed: 20179713]
15. Dodelet VC, Pasquale EB. Eph receptors and ephrin ligands: Embryogenesis to tumorigenesis. Oncogene. 2000; 19:5614–5619. [PubMed: 11114742]
16. Meyer S, Hafner C, Guba M, et al. Ephrin-B2 overexpression enhances integrin-mediated ECM-attachment and migration of B16 melanoma cells. Int J Oncol. 2005; 27:1197–1206. [PubMed: 16211213]
17. Nakada M, Anderson EM, Demuth T, et al. The phosphorylation of ephrin-B2 ligand promotes glioma cell migration and invasion. Int J Cancer. 2010; 126:1155–1165. [PubMed: 19728339]
18. Castellvi J, Garcia A, de la Torre J, et al. Ephrin B expression in epithelial ovarian neoplasms correlates with tumor differentiation and angiogenesis. Hum Pathol. 2006; 37:883–889. [PubMed: 16784989]
19. Huynh-Do U, Vindis C, Liu H, et al. Ephrin-B1 transduces signals to activate integrin-mediated migration, attachment and angiogenesis. J Cell Sci. 2002; 115:3073–3081. [PubMed: 12118063]
20. Alam SM, Fujimoto J, Jahan I, et al. Overexpression of ephrinB2 and EphB4 in tumor advancement of uterine endometrial cancers. Ann Oncol. 2007; 18:485–490. [PubMed: 17108150]
21. Tachibana M, Tonomoto Y, Hyakudomi R, et al. Expression and prognostic significance of EFNB2 and EphB4 genes in patients with oesophageal squamous cell carcinoma. Dig Liver Dis. 2007; 39:725–732. [PubMed: 17611172]
22. Yavrouian EJ, Sinha UK, Rice DH, et al. The significance of EphB4 and EphrinB2 expression and survival in head and neck squamous cell carcinoma. Arch Otolaryngol Head Neck Surg. 2008; 134:985–991. [PubMed: 18794445]
23. Kimura M, Kato Y, Sano D, et al. Soluble form of ephrinB2 inhibits xenograft growth of squamous cell carcinoma of the head and neck. Int J Oncol. 2009; 34:321–327. [PubMed: 19148465]
24. Ang KK, Harris J, Wheeler R, et al. Human papillomavirus and survival of patients with oropharyngeal cancer. N Engl J Med. 2010; 363:24–35. [PubMed: 20530316]
25. Shi S, Liu J, Joshi SB, et al. Biophysical characterization and stabilization of the recombinant albumin fusion protein sEphB4-HSA. J Pharm Sci. 2012; 101:1969–1984. [PubMed: 22411527]
26. Scehnet JS, Ley EJ, Krasnoperov V, et al. The role of Ephs, Ephrins, and growth factors in Kaposi sarcoma and implications of EphrinB2 blockade. Blood. 2009; 113:254–263. [PubMed: 18836096]
27. Kertesz N, Krasnoperov V, Reddy R, et al. The soluble extracellular domain of EphB4 (sEphB4) antagonizes EphB4-EphrinB2 interaction, modulates angiogenesis, and inhibits tumor growth. Blood. 2006; 107:2330–2338. [PubMed: 16322467]
28. Hasina R, Mollberg N, Kawada I, et al. Critical role for the receptor tyrosine kinase EPHB4 in esophageal cancers. Cancer Res. 2013; 73:184–194. [PubMed: 23100466]
29. Liu R, Ferguson BD, Zhou Y, et al. EphB4 as a therapeutic target in mesothelioma. BMC Cancer. 2013; 13:269. [PubMed: 23721559]

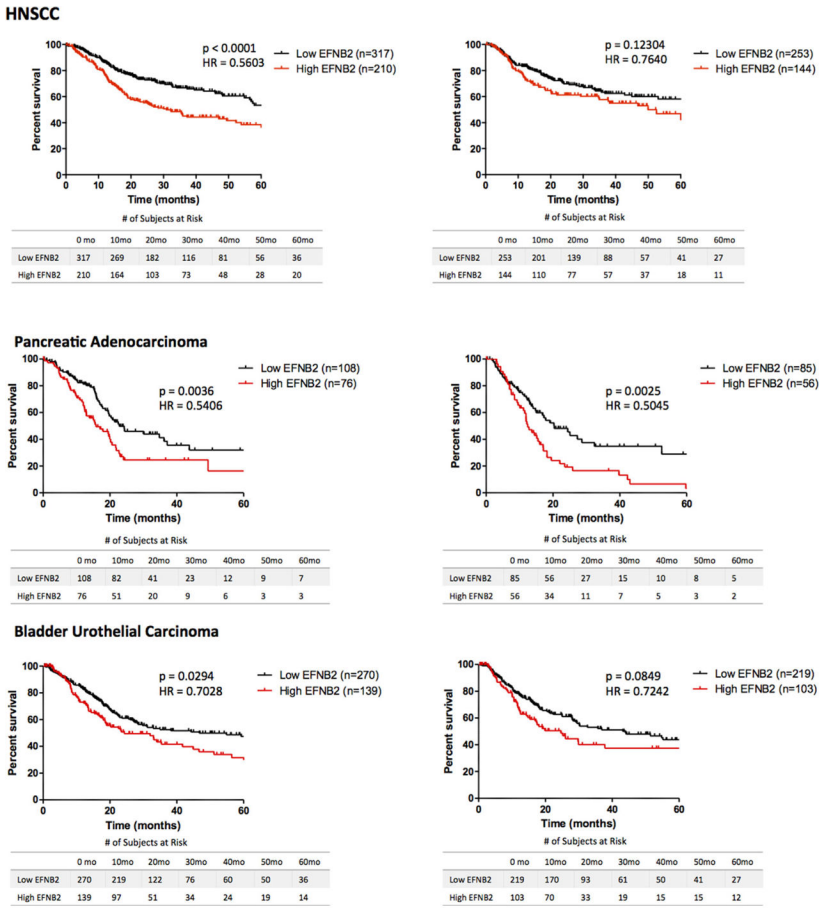

Figure 1.

EFNB2 expression is an indicator poor prognosis based on TCGA data in HNSCC (519 patients), pancreatic adenocarcinoma (186 patients), and bladder urothelial carcinoma (410 patients). Survival analysis and disease-free survival are based on average mRNA expression (high = above average; low = below average). Overall survival and disease-free survival was calculated by Kaplan–Meier method using log-rank tests for comparison. Disease-free survival (DFS) was defined as time from the date of diagnosis to the date of the last known occasion that the patient was disease-free, or the date of disease recurrence (local, regional, or distant recurrence). Death without documented recurrence was censored at the date of death. Univariate Cox proportional models were used to calculate the Hazard ratio (HR). Two-sided *P*-values are reported for all analyses.

A

HNSCC					
	High EFNB2		Low EFNB2		
Gender	**N**	**Frequency**	**N**	**Frequency**	***p-value***
Female	57	28%	80	25%	
Male	148	72%	236	75%	*0.5423*
Race					
Asian	4	2%	7	2%	
Black or African American	18	9%	29	10%	
White	177	89%	269	88%	*0.9607*
Primary Tumor Stage					
T1	7	3%	28	9%	
T2	62	31%	90	30%	
T3	60	30%	76	25%	
T4	73	36%	109	36%	*0.0546*
Age (years)					
Mean	60.3		61.2		
Median	60.0		61.0		*1.0000*
Alcohol Consumption					
0-3	32	30%	60	22%	
4-7	62	66%	67	53%	*0.0481**
Cigarette Smoking (Pack Years)					
0-10	12	11%	16	9%	
11-30	28	25%	52	28%	
>30	72	64%	117	63%	*0.7500*
HPV Status (p16)					
Positive	3	8%	36	48%	
Negative	33	92%	39	52%	*<0.0001**
Classification					
Oral Cavity	149	73%	167	53%	
Larynx	39	19%	77	24%	
Oropharynx	14	7%	66	21%	
Hypopharynx	3	1%	7	2%	*<0.0001**
TP53 Mutation	109/131	83.2%	92/146	63.0%	*0.0002**
EGFR Amplification (7p12)	32/201	15.9%	23/302	7.6%	*0.0052**

B

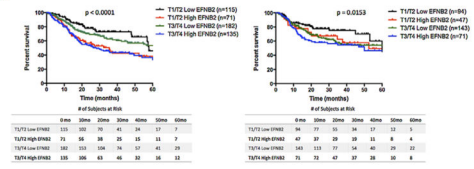

C

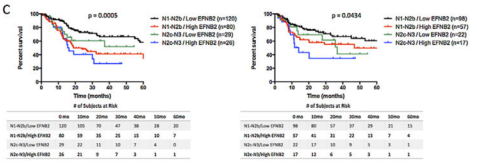

D

Multivariate
Cox proportional hazard modeling for survival (OC=Oral Cavity; OP=Oropharynx)

	OS			DFS		
	p-value	95% CI	HR	p-value	95% CI	HR
Alcohol	0.9708	0.5102-2.084	1.0131	0.0205	1.1890-8.6780	3.0989
EFNB2	0.0524	0.9930-4.310	2.0040	0.0374	1.0595-7.9210	2.7565
TP53	0.0839	0.8763-12.949	2.9580	0.2094	0.5660-20.13	2.9291
EGFR	0.1298	0.8173-3.993	1.8920	0.0345	1.1580-24.63	5.8829
Disease Site [OC/OP]	0.1469	0.7208-6.698	2.3640	0.3764	0.3212-11.845	2.3200
Disease Site [OC/Larynx]	0.5363	0.3461-1.660	0.7854	0.7966	0.3484-3.3732	1.1589

Figure 2.

Analysis of the HNSCC patient cohort based on EFNB2 expression. (A) Bivariate analysis of patient and tumor characteristics based on EFNB2 expression. *P*-values below 0.05 represent significant correlation between EFNB2 expression and the analyzed parameter. Two-sided Fisher's exact test and the Chiq-squared test were utilized for the analysis. Classifications of alveolar ridge, buccal mucosa, lip, oral tongue, and floor of mouth were re-classified to oral cavity. Tonsil was re-classified as oropharynx. (B) Subgroup analysis of HNSCC patients based on T-stage and (C) N-stage. (D) Multivariate Cox regression analysis for OS and DFS was performed for alcohol consumption frequency, TP53, EGFR, EFNB2, and disease site.

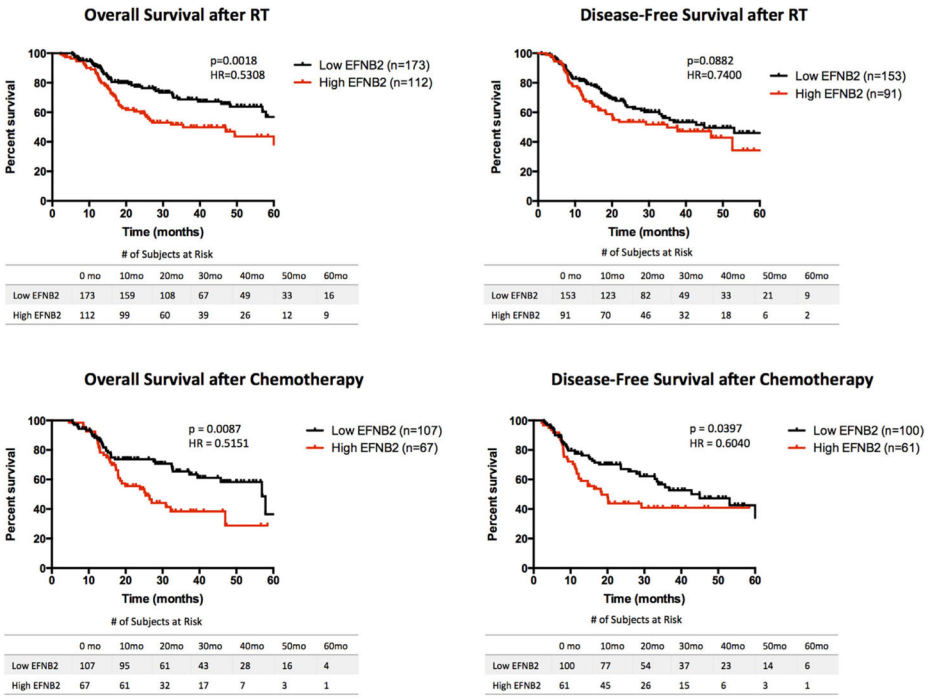

Figure 3.

High EphrinB2 expression in HNSCC patients correlates with worse response to radiotherapy (A) and chemotherapy (B). Only patients who received treatment for curative intent to the primary tumor were selected for analysis.

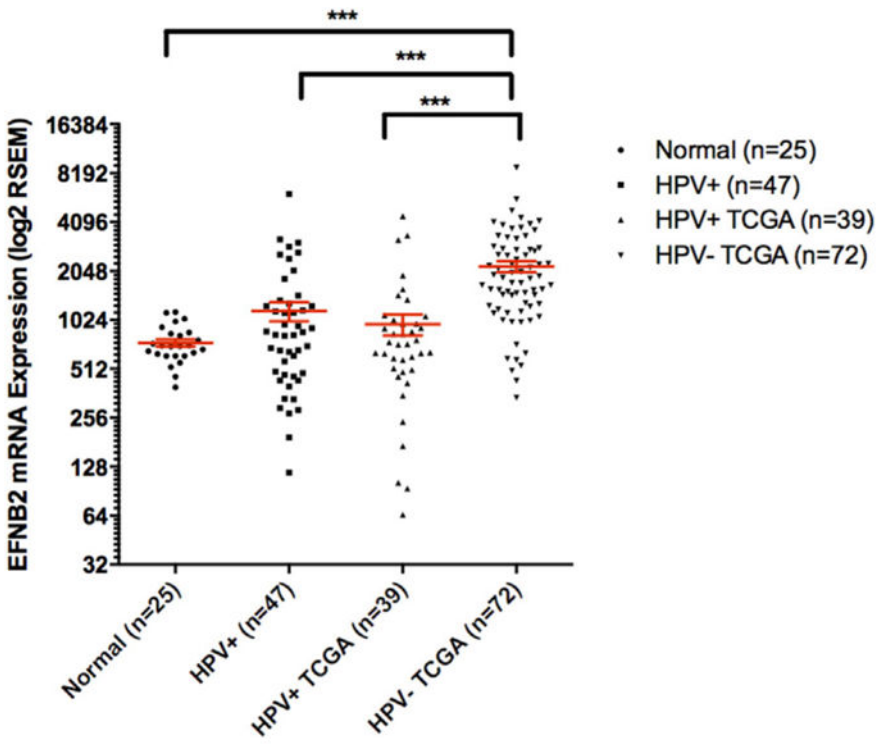

Figure 4.

Validation of the relationship between HPV status and EFNB2 expression. Sequencing data were pooled from patient data available from JHU and the TCGA. One way analysis of variance (ANOVA) with Tukey correction was applied for statistical analysis. Three stars represent *P*-value <0.0001.

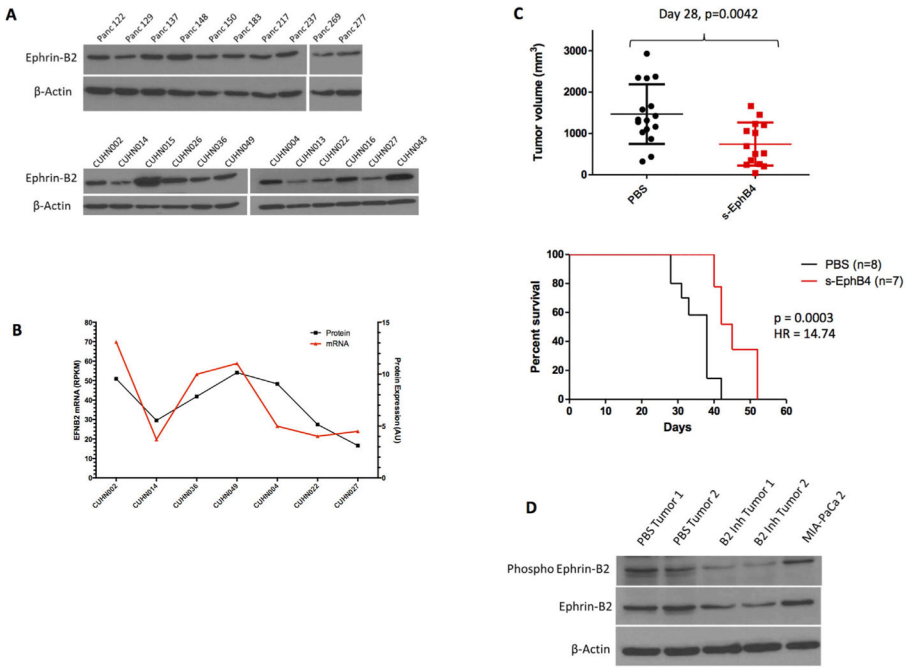

Figure 5.

EphrinB2 protein expression in HNSCC and pancreatic adenocarcinoma patient tissue. (A) Protein expression of EphrinB2 revealed through Western blot in 12 HNSCC and 12 pancreatic patient samples. (B) Correlation of mRNA to protein expression in seven HNSCC patient samples. (C) Treatment with s-EphB4-HSA of a HNSCC patient-derived xenograft from a patient with relapsed oral cavity cancer. (D) Early time point analysis showing effect of s-EphB4-HSA on total and phosphorylated levels of sEphB4-HSA.